American Mineralogist, Volume 89, pages 1067–1077, 2004

Isotopic and chemical alteration of zircon by metamorphic fluids: U-Pb age depth-profiling of zircon crystals from Barrow's garnet zone, northeast Scotland

CHRISTOPHER M. BREEDING,[1,†] JAY J. AGUE,[1,*] MARTY GROVE,[2] AND ANDREW L. RUPKE[3]

[1]Department of Geology and Geophysics, Yale University, New Haven, Connecticut 06520-8109, U.S.A.
[2]Department of Earth and Space Sciences, University of California, Los Angeles, California 90095-1567, U.S.A.
[3]Department of Geology and Geophysics, University of Utah, Salt Lake City, Utah 84112, U.S.A.

ABSTRACT

U-Pb isotopic analyses were done using ion microprobe depth-profiling on zircon crystals from Dalradian rocks in Barrow's garnet zone, northeast Scotland, to determine the timing of metamorphic fluid infiltration and investigate fluid-zircon interactions. Zircon crystals collected from altered metasedimentary rock adjacent to a cross-cutting quartz vein and from relatively unaltered, continuously equivalent layers distal to the vein indicate that Paleozoic fluid influx caused isotopic and chemical alteration along zircon crystal surfaces and internal fractures. "Ion drilling" into natural zircon crystal faces yielded U-Pb depth profiles with 50–100 nm spatial resolution that permitted U-Pb isotopic age analysis of thin grain rims affected by fluid-mediated growth/recrystallization at 500–550 °C. We interpret the measurements to indicate that fluid influx at 462 ± 8.8 Ma caused the growth/recrystallization of new zircon along pitted crystal surfaces and fractures in Archean zircon grains. Our age estimate overlaps the accepted age range (ca. 467–464 Ma) for peak Barrovian garnet growth, confirming that metamorphism and fluid influx were contemporaneous. The new zircon was enriched in U, Th, and common Pb relative to host grains, suggesting that U, Th, and Pb were actively transported by upper greenschist-facies metamorphic fluids. We present the first field-based evidence that common Pb in zircon can serve as an indicator of metamorphic fluid infiltration. Archean ages for some detrital zircons suggest contributions from a Lewisian/Scourian provenance.

INTRODUCTION

Evidence is widespread that crustal metamorphism is generally accompanied by fluid infiltration and that metamorphic fluids play important roles in mass and heat transfer, reaction kinetics, ore deposition, and mineral assemblage distribution and preservation (e.g., Rye and Rye 1974; Rye et al. 1976; Rumble et al. 1982; Chamberlain and Rumble 1988; Baumgartner and Ferry 1991; Bickle 1992; Dipple and Ferry 1992; Yardley and Bottrell 1992; Ague 1994; Ague 1997; Ingebritsen and Manning 1999; Breeding and Ague 2002; Breeding et al. 2003; Wing and Ferry 2003). A thorough understanding of the chronological relationship between metamorphism and fluid infiltration is critical in deciphering the history of ancient metamorphic terranes and mountain belts. Nevertheless, constraining the timing of metamorphic fluid infiltration has proven difficult largely because interactions between metamorphic fluids and important geochronometers like zircon are complex (Ayers and Watson 1991; Sinha et al. 1992; Konzett et al. 1998; Högdahl et al. 2001; Carson et al. 2002).

This paper focuses on zircon samples from upper greenschist-facies Dalradian metasedimentary rocks of Barrow's classic garnet zone in northeast Scotland. Our primary goals are as follows: (1) Develop a unique geochronological technique for precisely dating metamorphic fluid infiltration. Metamorphic fluids had a significant impact on the growth of index minerals like garnet in Scotland (Ague 1997) and affect the chemical and mineralogical development of most metamorphic terranes. (2) Constrain the chemical and isotopic processes that cause U-Pb age discordance in zircon by investigating sub-micrometer scale compositional changes. (3) Use field-based data to establish common Pb in zircon as an indicator of fluid-rich metamorphic conditions. (4) Investigate the initial crystallization ages of detrital Dalradian zircon crystals to constrain provenance and determine whether the effects of greater zircon age (e.g., radiation damage) influence isotopic alteration. To address these issues and deal with the difficulties introduced by heterogeneous detrital grain age populations, zircon crystals were analyzed with the ion microprobe. Analyses were obtained by standard ion drilling into conventionally sectioned and polished grains as well as depth-profile drilling into original, unprocessed grain surfaces (e.g., Grove and Harrison 1999; Carson et al. 2002; Mojzsis and Harrison 2002).

Typical ion probe or SIMS (Secondary Ion Mass Spectrometry) analysis allows for a lateral spatial resolution of ~10–40 μm (pit depth of ~0.25–0.50 μm) for zircon U-Pb age determinations (Compston et al. 1984). Isotopic analysis at this scale can avoid many of the multi-grain and domain mixing problems that impact conventional U-Pb techniques (Mezger and Krogstad 1997). Isotopic alteration of zircon by metamorphic fluids, however, can occur at micrometer and sub-micrometer

* E-mail: jay.ague@yale.edu
† Present Address: Gemological Institute of America, 5345 Armada Dr., MS 33, Carlsbad, CA 92008.

scales (Zeitler et al. 1989; Chamberlain et al. 1995; Carson et al. 2002). Because ion drilling rates into zircon are relatively slow (several micrometers per hour), it is potentially possible to obtain extremely high spatial resolution (tens of nanometers) analyses that are geologically meaningful if the measurements are performed normal to a reaction front for fluid interaction (i.e., original grain boundaries). SIMS analysis is the only currently available technique capable of detecting sub-micrometer isotopic changes within zircon grains. Carson et al. (2002) previously documented metamorphic, fluid-induced isotopic resetting/recrystallization within 0.2 μm of original zircon grain boundaries (see also Mojzsis and Harrison 2002). The results of Carson et al. demonstrated that this type of depth-profile analysis was capable of yielding a continuous, internally consistent, high-resolution record of isotopic and chemical changes from outer grain surfaces to zircon subsurface regions (i.e., the deepest depth-profile analysis). Hence, it is clear that combination of polished-grain and depth-profile modes of analysis can provide a multi-scale, chemical and isotopic description of a zircon grain and allows for direct comparison of fluid processes affecting zircon crystals collected from different parts of a sample.

We have analyzed both original zircon grain boundaries and conventionally sectioned and polished zircon crystals collected from a continuous sequence of Dalradian metasedimentary rock layers crosscut by a metamorphic quartz vein in an effort to determine the timing of metamorphic fluid influx in Barrow's garnet zone. Chemical and isotopic profiles for zircon grains adjacent to the vein were compared with profiles for zircon crystals occurring distal to the vein to assess the impact of infiltrating fluids on zircon compositions. Our SIMS analysis utilized material previously studied by Ague (1997) for bulk-chemical analysis to provide an internally consistent geochemical framework for zircon study.

GEOLOGIC SETTING

Dalradian metasediments

Our investigation of metamorphic fluid alteration of zircon focuses on metasedimentary rocks of the Dalradian Supergroup, south of Aberdeen, on the northeastern coast of Scotland (Fig. 1). Dalradian schists cover a wide region of northern Scotland and Ireland that is bounded to the north and south by the Great Glen and Highland Boundary (HBF) faults, respectively. The sequence consists of late Proterozoic to early Paleozoic sediments that were deposited on the continental shelf of Laurentia during the opening of the Iapetus Ocean and subsequently metamorphosed during arc accretion (Grampian Orogeny) and closure of the ocean basin in the early Paleozoic (Atherton 1977; Harte et al. 1984; Oliver et al. 2000; Oliver 2001; Baxter et al. 2002). Deformation and recrystallization associated with the Grampian Orogeny resulted in an increase in metamorphic grade across the terrane from greenschist facies adjacent to the HBF to amphibolite facies further north. Metamorphic mineral assemblages from this region in Scotland inspired Barrow's classic regional metamorphic index mineral zone concept (Barrow 1893; Barrow 1898; Barrow 1912; Chinner 1967; Atherton 1977). Recent geochemical and geochronological investigations near Stonehaven and Glen Clova have revealed that metamorphic fluids and igneous intrusions contributed to the development of the Barrovian index minerals (Ague 1997; Baxter et al. 2002). Peak metamorphic conditions in the sillimanite zone near Glen Clova were ~650–700 °C and ~6 kbar (Ague et al. 2001), whereas metamorphism and fluid infiltration in the garnet zone south of Aberdeen occurred at ~535 °C and ~3.8–4.5 kbar (Droop and Harte 1995; Ague 1997) (Fig. 1).

Timing of Barrovian metamorphism

The timing of peak Grampian metamorphism in the Barrovian type locality in northeast Scotland has proven difficult to resolve. Application of various dating techniques and interpretations of field-based criteria have generated a wide range of age estimates for the timing of metamorphism (see summary in Baxter et al. 2002). However, recent dates for peak metamorphic garnet growth in the region have provided important new constraints. Oliver et al. (2000) obtained Sm/Nd garnet ages ranging from 472 to 467 Ma from the Barrovian kyanite and garnet zones. By combining these age estimates with their own new Sm/Nd garnet ages and associated textural relations, Baxter et al. (2002) documented an early stage of garnet growth at 473 Ma, but determined that peak metamorphic garnet growth under garnet, kyanite, and sillimanite zone conditions most likely occurred at ca. 467–464 Ma. These data provide the most reliable, currently published ages for peak Barrovian metamorphism and garnet growth in northeast Scotland. We obtain a precise age for fluid infiltration and compare this age with the timing of Barrovian metamorphism in the garnet zone (Ague 1997).

Geochemical and petrologic background

The sample analyzed in this study (JAB 101L) was collected from the belt of "spotted" chloritoid schists within the classic garnet zone south of Aberdeen (Barrow 1898; Fig. 1). Geochemistry of the rock layers was previously described by Ague (1997). The "spotted" schists are so named for abundant ellipsoidal plagioclase porphyroblasts that likely formed during greenschist-facies, garnet-zone conditions (Ague 1997; and references therein). Quartz veins are common throughout the schist belt and occur mainly in boudin necks and at lithologic contacts. Veins in the study area occupy ~13 vol% of the rock mass and have a geometric mean width of ~3 cm (Ague 1997). Specimen JAB 101L contains primary sedimentary layering defined by pelitic, semipelitic, and psammitic layers that are cross-cut at a high angle by a quartz vein in a boudin neck at one end of the sample (Fig. 2). The quartz vein also contains minor pyrite and retrograde chlorite. Metasedimentary layers in the altered region (or "selvage") adjacent to the vein contain quartz + plagioclase + chlorite + biotite + almandine-rich garnet ± muscovite ± rutile ± pyrite. Those away from the vein contain abundant muscovite and chloritoid, much less plagioclase, and no garnet. Zircon is ubiquitous in all parts of the sample. Plagioclase spots and garnet porphyroblasts at this locality become larger and more abundant adjacent to the quartz veins, suggesting a genetic link between prograde fluid infiltration and the growth of metamorphic minerals. Ague (1997) reported that metamorphic fluid infiltration was accompanied by an increase in Na, Ca, and Sr, and a decrease in K and Rb in altered metasediments adjacent to the quartz vein, relative to less altered metasediments distal to the vein (Fig. 2). These geochemical systematics are reflected in mineralogical

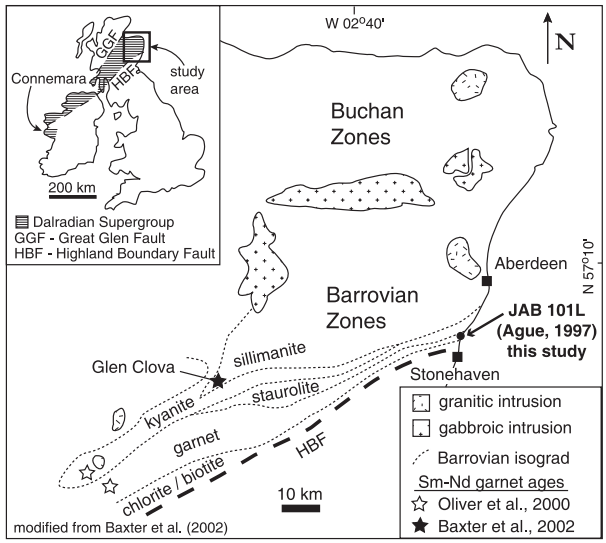

FIGURE 1. Map of study area in northeast Scotland showing Barrovian mineral zones adjacent to Highland Boundary Fault (HBF) and igneous rock distribution. Dalradian rocks extend across Scotland and Ireland and include Connemara schists. Stars indicate sample locations for published Sm-Nd whole-rock garnet ages. Sample for this study, JAB-101L, collected from garnet zone south of Aberdeen and geochemically characterized by Ague (1997).

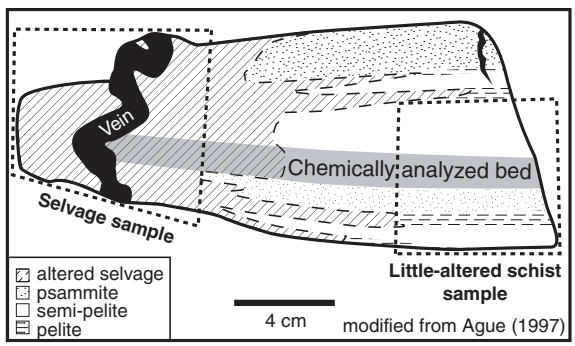

FIGURE 2. Diagram of JAB-101L study sample. Sample consists of metamorphosed interlayered psammite, pelite, and semi-pelite with cross-cutting quartz metamorphosed vein at one end. Altered rock adjacent to vein (selvage) extends along layering to various widths depending on lithology. Geochemically analyzed semi-pelite layer of Ague (1997) shown in gray. Selvage and little-altered schist sub-samples used in this study marked by dashed boxes.

changes in the fluid-altered rock. Adjacent to the quartz vein, fluid infiltration facilitated growth of plagioclase, destruction of muscovite, and stabilization of garnet by altering the bulk composition of the rock (Ague 1997). Previously unpublished trace-element data also indicates that Pb was added adjacent to the vein (Fig. 3; Table 1)[1]. Some fluid infiltration likely oc-

[1] For a copy of Tables 1, 2, 3, 4, 5, and 6, Document item AM-04-067, contact the Business Office of the Mineralogical Society of America (see inside front cover of recent issue) for price information. Deposit items may also be available on the *American Mineralogist* web site at http://www.minsocam.org.

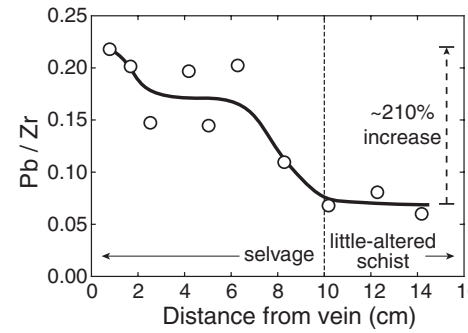

FIGURE 3. Whole-rock geochemical Pb data metamorphosed for semi-pelite layer from Figure 2. Ratios of Pb concentrations to Zr reference frame (Table 1)[1]. Dashed line at x = 10 cm indicates boundary between vein selvage and relatively unaltered semi-pelite as defined by Ague (1997). Pb was added (~200%) within vein selvage relative to rock >10 cm from vein.

curred in parts of the layers more distal to the veins as well; however, the relative absence of significant chemical alteration in metasediments distal to the vein indicates that fluid interactions were much less intense than those within the vein selvage. The occurrence of plagioclase spots in the sample serves as a distinct marker of the extent of fluid alteration. Altered zones adjacent to the vein vary in width depending on the lithology from 2–3 cm wide in psammitic layers to 6–8 cm wide in semipelitic layers to 10–15 cm wide in pelitic layers (Ague 1997). The well-defined distinction between fluid-altered rock and relatively unaltered metasediments, combined with the existing geochemical framework, makes this an ideal setting in which to investigate the interactions between upper greenschist-facies metamorphic fluids and the isotopic systematics preserved in zircon crystals.

METHODS

Sample preparation

The clear mineralogical distinction between altered selvage and relatively unmetasomatized metasediment prompted us to examine two subregions of sample JAB 101L. One subregion included the quartz vein and the most intensely altered metasediments adjacent to the vein. We refer to this as the "selvage" (Fig. 2). The other is termed the "little-altered schist", and includes relatively unaltered metasediments distal to the vein that contain few plagioclase spots (Fig. 2).

Each subregion of JAB 101L was crushed and processed independently using standard density and magnetic methods to concentrate zircon and other heavy minerals. Zircon crystals were hand-selected with the aid of a binocular microscope. A number of the zircon crystals and standards were mounted on double-sided tape, potted in epoxy, sectioned, polished, cleaned ultrasonically, and coated with Au. Zircon grains that possessed the most readily identifiable crystal faces were reserved for depth-profile analysis. The natural crystal faces of these grains were oriented parallel to the mounting surface. A previously polished block of standards was included in the mount. The composite sample was potted in epoxy, cleaned ultrasonically, rinsed in 1 *N* HCl to reduce surficial common Pb contamination, and coated in Au with no polishing performed.

Ion microprobe (SIMS) analysis

Ion microprobe U-Pb analyses of zircon were obtained with the Cameca IMS 1270 at the University of California, Los Angeles using previously published analytical techniques (Grove and Harrison 1999; Mojzsis and Harrison 2002). Secondary ions were sputtered using an aperture-defined (i.e., Kohler illumination), 12 nA, 12.5 keV, O^- primary beam. Secondary positive ion beams corresponding to $^{94}Zr_2{}^{16}O$, ^{204}Pb, ^{206}Pb, ^{207}Pb, ^{208}Pb, ^{232}Th, ^{238}U, and $^{238}U^{16}O$ were measured in peak hopping mode. Calculation of U-Pb ages was accomplished using UCLA (ZIPS v2.4 written by C.D. Coath 2000) and ISOPLOT v2.49 (Ludwig 2001) software pack-

ages. Pb isotopic ratio corrections were made using ^{204}Pb as a proxy for common Pb content ($^{206}Pb/^{204}Pb = 16.2$; $^{207}Pb/^{204}Pb = 15.35$). The composition of common Pb was estimated from the model of Stacey and Kramers (1975). The Pb/U relative sensitivity factors for individual analyses were determined from a linear working curve constructed from concurrent measurements of AS-3 standard zircon ($^{206}Pb/^{238}U$ age of 1099 Ma; Paces and Miller 1993). Uranium, Th, and ^{204}Pb concentrations were estimated semi-quantitatively by comparing $U/^{94}Zr_2{}^{16}O$, $Th/^{94}Zr_2{}^{16}O$, and $^{204}Pb/^{94}Zr_2{}^{16}O$ in the unknowns to analogous ratios measured from AS-3 standard zircon. Concentration data for U and Th in AS-3 were obtained from new electron microprobe analyses (Table 2)[1] and data previously presented in Paces and Miller (1993). Pb concentrations in AS-3 were based entirely upon the results of Paces and Miller (1993). Note that electron microprobe analysis was employed to verify reasonable ranges of U and Th concentrations in several unknown zircon crystals (Table 2)[1]. Error ellipses shown in all figures reflect 1σ standard errors, whereas intercept ages are given at 2σ. Analyses of conventionally sectioned and polished zircon involved ~12 minutes total counting time and formation of sputter pits that were ~20–25 μm in diameter. Depth-profile analysis of unpolished original grain surfaces involved longer counting times (~32–65 minute per analysis) and wider sputter pits (30–40 μm diameter). A field aperture smaller than the secondary beam diameter was employed to improve depth resolution by excluding secondary ions derived from the periphery of the analysis pit. Analysis craters were consistently flat bottomed and ranged in depth from 2.1–4.3 μm, as measured using a MicroXAM scanning interferometer with MapVue software at Yale University (Luttge et al. 1999).

Imaging and electon microprobe analysis

Zircon U and Pb concentration measurements, secondary electron imaging (SE), back-scattered electron imaging (BSE), and cathodoluminescence imaging (CL) were performed at Yale University using a JEOL JXA-8600 electron microprobe equipped with wavelength dispersive spectrometers and a Gatan mini-CL detector. Natural and synthetic standards, off-peak background corrections, and $\phi(\rho z)$ matrix corrections were used for mineral analyses. Analytical conditions for zircon analyses were 15 kV accelerating voltage, 50 nA beam current, and a 20 μm beam spot. The beam spot size was selected to approximate that used for ion-microprobe analyses. Analytical count times for U and Th were 450 sec (on-peak) and 225 sec (high and low off-peak backgrounds).

POLISHED-GRAIN VS. DEPTH-PROFILE ANALYSIS

Polished-grain SIMS analysis

For the polished-grain analysis, 63 spots on 38 zircon grains were analyzed for U and Pb isotopic composition using the ion microprobe. Twenty grains were from the vein selvage and 18 were from the little-altered schist (Fig. 2; Tables 3–4) [1]. Samples were selected randomly from each subregion of JAB 101L and consisted of euhedral and subhedral grains of various sizes (all ≥30 μm in width to facilitate ionprobe analysis). Both optically transparent and opaque (brown) grains were included.

Isotopic measurements revealed concordant and discordant data for zircon crystals in both the selvage and little-altered schist (Fig. 4A). Grains yielding "concordant" U-Pb systematics define a near-continuous array of ages. These relations are not unexpected, as variability of the source terrains from which the detrital grains originated and/or metamorphic recrystallization likely resulted in the range of preserved ages. Ten zircon grains (16 spots) define a near concordant array of Archean $^{207}Pb/^{206}Pb$ ages ranging from 2850 to 2550 Ma. These Archean ages documented from the Dalradian metasediments (e.g., Cathwood et al. 2003) possibly represent sedimentary contributions from a Lewisian/Scourian source region. Two grains (2 spots) occur with $^{207}Pb/^{206}Pb$ ages of ~1840 Ma. Fifteen grains (20 spots) have $^{207}Pb/^{206}Pb$ ages spanning 1460–870 Ma. Many of these ~1000 Ma zircon crystals were mostly likely derived from a Grenvillian source region, indicating the second major sediment provenance for the Dalradian metasediments in northeast Scotland. Source terrane contributions to the Dalradian will be addressed in greater detail in a subsequent paper. Five grains (5 spots) yield Latest Proterozoic to Paleozoic $^{207}Pb/^{206}Pb$ ages of 660–300 Ma. The discordant data (20 spots from 15 grains) all plot along a well-defined array between the Archean age cluster and the Paleozoic age cluster (Fig. 4B). Although it is impossible to evaluate quantitatively the extent of Pb loss affecting the weakly discordant 1460–870 Ma zircon population, it is evident that the older Archean zircon crystals were much more susceptible to an apparent loss of Pb in the Paleozoic than the younger grains (Figs. 4A and 4B). Inasmuch as peak Barrovian metamorphism in Scotland has been dated at 467–464 Ma, we focus further discussion upon the array of discordant data and the end-member Archean and Paleozoic concordant populations.

The detrital origin of the Dalradian zircon crystals makes it inappropriate to calculate upper and lower intercepts for the discordant array. However, the fact that all discordant analyses fall within an envelope defined by the age spreads of the Archean and Paleozoic concordant age groups (Fig. 4B) suggests that the data can be interpreted qualitatively in this manner. A best-fit discord for the data array indicates a lower intercept at 507 ± 82 Ma and an upper intercept at 2724 ± 26 Ma. Although error in the intercepts must partially reflect the detrital origin of the grains, the protolith clearly contains a strong Archean age component. Moreover, the lower intercept overlaps the accepted Barrovian metamorphic age range within error.

Depth-profile SIMS analysis

To obtain a more precise fluid-infiltration age, fourteen analyses were performed on 11 unpolished zircon grains using the higher resolution, depth-profile methods previously employed by Grove and Harrison (1999), Carson et al. (2002), and Mojzsis and Harrison (2002). Six of the grains were from the selvage and five from the little-altered schist (Tables 5–6) [1]. Zircon U-Pb age systematics from subsurface regions are similar for both parts of sample JAB 101L. Zircon crytals yielding 800–1000 Ma U-Pb ages are concordant (or nearly concordant) through the depth range analyzed with no evidence for alteration at the crystal surfaces (Figs. 5A

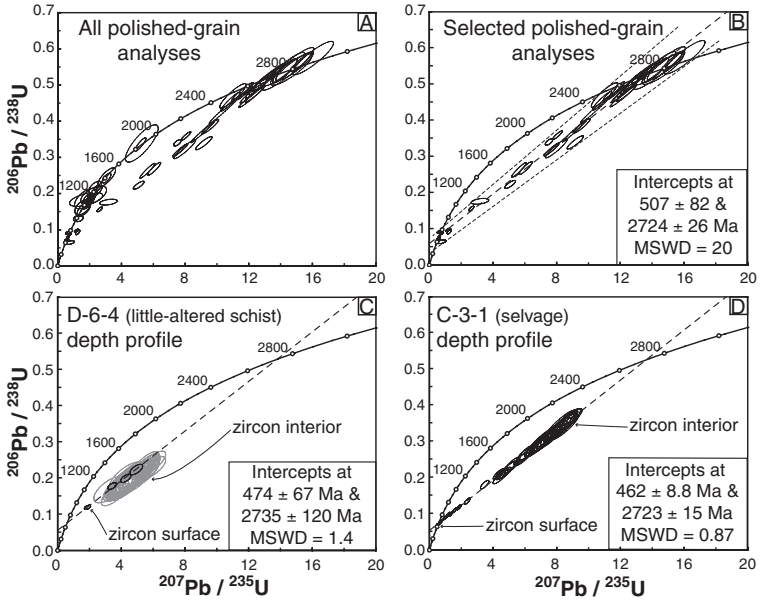

FIGURE 4. U-Pb concordia plots for polished-grain **(A-B)** and representative depth-profile analyses **(C-D)**. Error ellipses shown at 1σ. Regression lines and intercepts at 2σ. Concordia ages given in Ma. **(A)**. All polished-grain data with radiogenic $^{206}Pb \geq 92.0\%$. **(B)**. Concordant Archean and Paleozoic age groupings and discordant data from A. Linear regression (long-dashed line) for entire data set defines upper and lower intercepts. Short-dashed lines connect age limits of two concordant populations. Note that all discordant data plot within envelope defined by short-dashed lines. **(C)**. Depth-profile analysis D-6-4 from little-altered schist. Linear regression for data from altered, outer 0.35 μm of zircon rim (black ellipses; $n = 4$) defines intercept ages. Grain subsurface data (gray ellipses) excluded from regression due to large errors. **(D)**. Depth-profile analysis C-3-1 from vein selvage. Note near-continuous array of data from grain surface to subsurface regions. Linear regression yields precise upper and lower intercept ages.

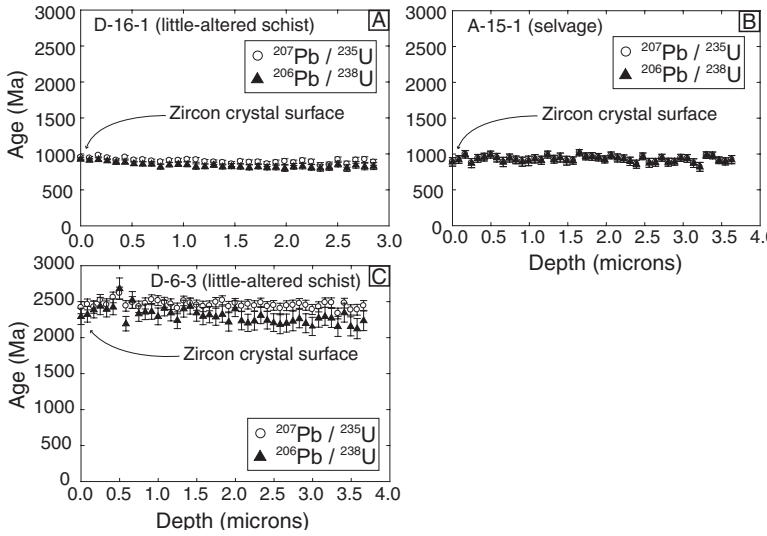

FIGURE 5. Isotopic age vs. depth plots for depth-profiled zircon crystals. Error bars at 1σ. **(A-B)**. Representative ~1000 Ma zircon crystals from little-altered schist (A) and vein selvage (B). Note lack of discordance and absence of surface alteration. **(C)**. Rare, mostly concordant, older zircon (~2400 Ma) from little-altered schist. Note lack of surface alteration. Older, unaltered zircon crystals were not observed in the selvage. Offset between $^{207}Pb/^{235}Pb$ and $^{206}Pb/^{238}U$ ages correlates with degree of discordance.

and 5B). These zircon crystals are commonly colorless and transparent. Older zircon crystals, which are commonly opaque and brown, can also preserve near-concordant ages (~2400–2500 Ma; Fig. 5C). More typically, however, subsurface regions within the older zircon crystals yield homogeneous, yet highly discordant Archean U-Pb ages. Unlike the 800–1000 Ma zircon crystals, grain surfaces and cracks within the 2400–2500 Ma zircon crystals show significant isotopic differences from interior subsurface regions. Although the extent of grain surface U-Pb age discordance occurs at different length scales in the selvage and little-altered schist (see below), concordant Paleozoic ages are always approached at the lower intercept. Upper intercepts obtained for all depth-profiled zircon crystals are consistent with the age groupings observed in the polished-grain analyses (Fig. 4A). In particular, opaque brown zircon crystals yield ~2630–2800 Ma upper intercept ages.

The scale of alteration in the near-surface regions of zircon crystals from the selvage and little-altered schist varies significantly. Results from several depth-profile analyses illustrate the differences (Figs. 6A, 6B, 6C, and 6D). Two representative analyses, C-3-1 (selvage, Fig. 4D) and D-6-4 (little-altered schist, Fig. 4C), will be discussed in greater detail. The analyses were performed on grains that yield highly discordant U-Pb ages from interior subsurface regions and Archean upper intercept ages. Zircon crystals from both subregions of JAB 101L show indications of Paleozoic isotopic alteration at grain surfaces and/or along fractures (Figs. 4C and 4D; Figs. 6C and 6D). However, the length scale of isotopic modification was significantly greater for the zircon situated adjacent to the vein (selvage) than it was for the distal zircon (little-altered schist). Specifically, the C-3-1 selvage zircon analysis revealed isotopic alteration both at the surface and along a large cross-cutting internal fracture that was intersected at depths of 1.1–2.0 μm beneath the grain boundary (Fig. 6D). Isotopic alteration of the grain surface penetrated to a depth of ~1.3 μm within the selvage zircon. In contrast, results from the distal, little-altered schist zircon (D-6-4) revealed no U-Pb istopic disturbance at depths greater than ~0.35 μm beneath the surface and no evidence for isotopic alteration along internal fractures (Fig. 6C).

Geochemical changes associated with isotopic alteration at grain surfaces provide clues about the nature of infiltrating fluids and further illustrate the different length scales of alteration in the selvage and little-altered schist zircon crystals. Significant enrichment of U, Th, and common Pb (^{204}Pb) occurs at the surface of the selvage zircon crystals. In the case of C-3-1, U concentration decreases from 3550 ppm at the surface to 330 ppm at positions furthest from the grain boundary. Decreases are also found for Th (2600 to 160 ppm) and ^{204}Pb (0.69 to 0.07 ppm) (Figs. 7A, 7B, and 7C). Interestingly, Th/U ratios at the grain boundaries (0.73) are neither markedly low (i.e., <<1) nor significantly different than those from the interior (0.48) (cf., Mozjsis and Harrison 2002). Within the cross-cutting fracture in the selvage zircon, U, Th, and ^{204}Pb concentrations are also elevated (715 ppm, 980 ppm, and 0.25 ppm respectively; see Figs. 7A, 7B and 7C). Concentrations of ^{204}Pb within the internal cross-cutting fracture do not correlate with measured values for ^{197}Au (added to grain surfaces during Au-coating preparation), indicating that the observed enrichments in common Pb are related directly to chemical and isotopic alteration and are not the result of sample contamination. Consistent, though less-pronounced patterns of surface enrichment of U, Th, and ^{204}Pb also occur for zircon from the little-altered schist. In the case of D-6-4, U concentrations decrease from 950 ppm at the surface to 40 ppm at depth. Similarly, Th decreases from 390 to 75 ppm and ^{204}Pb decreases from 0.14 ppm to <0.01 ppm (Figs. 7A, 7B, and 7C). Although Th/U values at the grain boundary (0.41) and in the interior (1.88) differ somewhat, they are of overall similar magnitude to Th/U values determined for the selvage zircon. Concurrent enrichment of U and Th in both the selvage and little-altered schist suggests that Th/U ratios were controlled by the fluid chemisty rather than by ambient metamorphic *P-T* conditions, resulting in variable Th/U values. The fact that $^{94}Zr_2{}^{16}O$ intensities remained constant throughout the ion microprobe depth profiles indicates that material encountered during ion drilling was zircon. This conclusion has been further confirmed by electron microprobe analyses. In zircon crystals from both the selvage and little-altered schist, length scales of chemical alteration are nearly identical to those for isotopic alteration, indicating that the chemical and isotopic changes were contemporaneous.

INTERNAL AND SURFICIAL ZIRCON STRUCTURES

CL, BSE, and SE imaging of polished, sectioned zircon crystals and natural crystal surfaces from depth-profiled zircon crystals provide additional information regarding the isotopic alteration. Zircon crystals examined from both subregions of JAB 101L have well-defined oscillatory zoning of igneous cores with concordant Archean ages measured on sectioned and polished grains (Connelly 2000; Fig. 8A). In grains from the selvage, zircon cores with oscillatory zoning are commonly mantled and/or truncated by narrow rims of uniform, brightly CL-luminescent zircon with variably discordant U-Pb isotopic compositions and high concentrations of U, Th, and ^{204}Pb (Figs. 8A and 8B). Elevated U concentrations are not typically associated with CL brightness, so a different CL activator like Dy may be responsible (Hanchar and Rudnick 1995). Qualitative EDS (energy dispersive spectrometry) analysis suggests significant Dy concentrations near the surfaces of selvage zircon crystals. As discussed above, discordant U-Pb age results from the bright regions are always consistent with a lower concordia intercept of Paleozoic age (Fig. 4B). Zircon crystals from the little-altered schist rarely exhibit CL-bright rims in polished grains, but locally show thin, bright rims on natural surfaces (Fig. 8D). SE imaging of natural crystal surfaces on depth-profiled grains offers a detailed view of the zircon rim texture and indicates that the outer rims are very irregular, containing abundant pits and fractures (Fig. 8E).

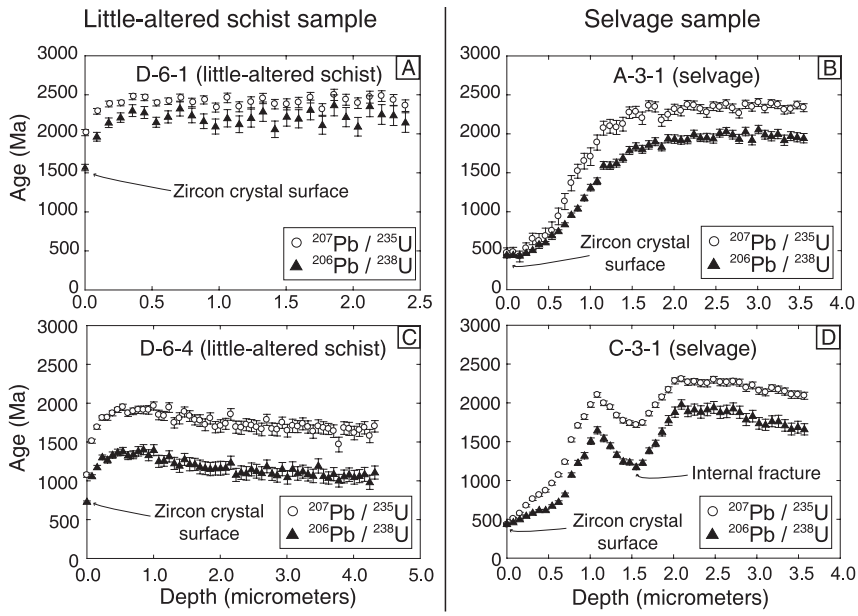

FIGURE 6. (A-D). Representative zircon crystals (older than 1000 Ma) from little-altered schist (A, C) and selvage (B, D). Note significant subsurface discordance in all grains. Selvage zircon crystals show intense isotopic alteration at crystal surfaces to depths of ~1.3 μm with outermost surface concordant at ~462 Ma. Internal fracture in selvage zircon analysis C-3-1 (D) also shows isotopic trend approaching younger age. Little-altered schist zircon crystals show less intense isotopic alteration at surfaces to depths of ~0.35 μm. Outermost zircon surfaces are discordant, but trend toward Paleozoic ages. Zircon grains D-6-4 (C) and C-3-1 (D) used for geochemical analysis (see Fig. 7).

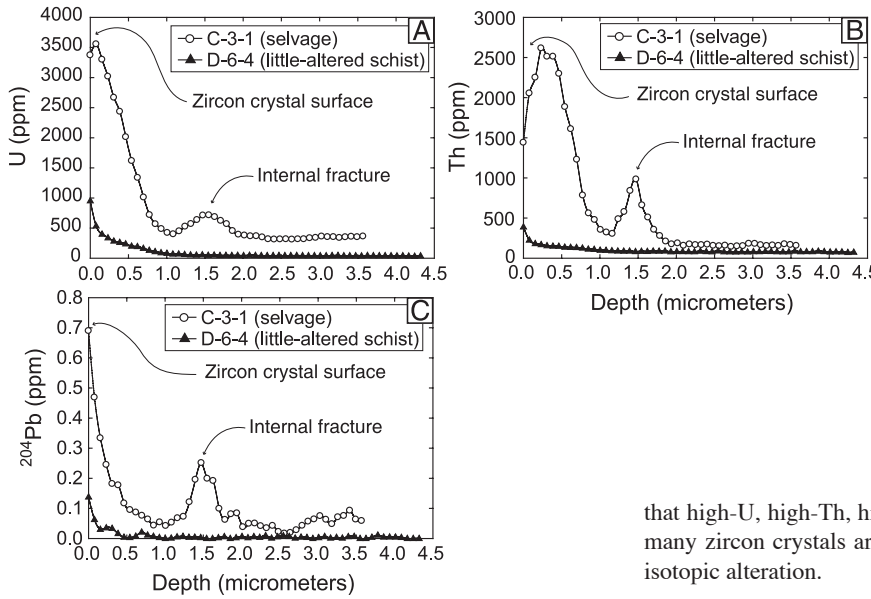

FIGURE 7. (A-C). U, Th, and ^{204}Pb vs. depth plots for depth-profiled zircon crystals C-3-1 (selvage) and D-6-4 (little-altered schist). ^{204}Pb used as proxy for common Pb in zircon. Geochemical concentrations are semi-quantitative (Paces and Miller 1993), but consistent with concentrations obtained by electron microprobe analysis (Table 2) [1]. Note increases in all elements at zircon surfaces and along internal fracture (C-3-1). Elemental increases are significantly more intense and occur over longer length scale in grain from vein selvage (C-3-1) than in little-altered schist zircon crystals (D-6-4).

Patchy subsurface zones of relatively low-luminescent zircon (Figs. 8B and 8C) in grains from both sub-samples also yield partially discordant age data and probably represent the uniform, highly discordant ages noted earlier for the subsurface sections of depth-profile analyses of many Archean zircon crystals (Figs. 6A, 6B, 6C, and 6D). Unlike the oscillatory zoned older concordant zircon cores, grains with near-concordant, mostly Paleozoic, ages (660–300 Ma) are non-luminescent and contain inclusions of quartz and feldspars along crystallographic growth planes.

To summarize, depth-profile analysis reveals that the isotopic alteration of the Archean grains occurred mainly at crystal surfaces (< 1.3 µm deep for selvage grains; < 0.35 µm deep for grains from the little-altered schist) and along fractures (Figs. 6A, 6B, 6C, and 6D). Imaging (CL, BSE, and SE) of ion microprobe pits confirms the variable (generally sub-micrometer) length scales of the alteration (Figs. 8C and 8D) and indicates that high-U, high-Th, high-^{204}Pb, brightly luminescent rims on many zircon crystals are the result of Paleozoic chemical and isotopic alteration.

DISCUSSION

The timing of metamorphism and fluid alteration

Sub-micrometer-scale depth-profiling of altered zircon is a highly underutilized geochronological tool for dating metamorphic events (e.g., Mozjsis and Harrison 2002) and affords a unique opportunity to determine precisely the timing of metamorphic fluid infiltration (e.g., Carson et al. 2002). Depth-profile analysis of zircon in the present study provides important insights regarding the timing of metamorphism and fluid infiltration of Dalradian metasedimentary rocks. For example, depth profiling results from a zircon grain in the vein selvage (C-3-1) yield a tight discord fit with a Paleozoic lower intercept age at 462 ± 8.8 Ma. The precision of this lower intercept age estimate is comparable to other metamorphic age estimates for the region and represents the age of Barrovian metamorphic fluid alteration

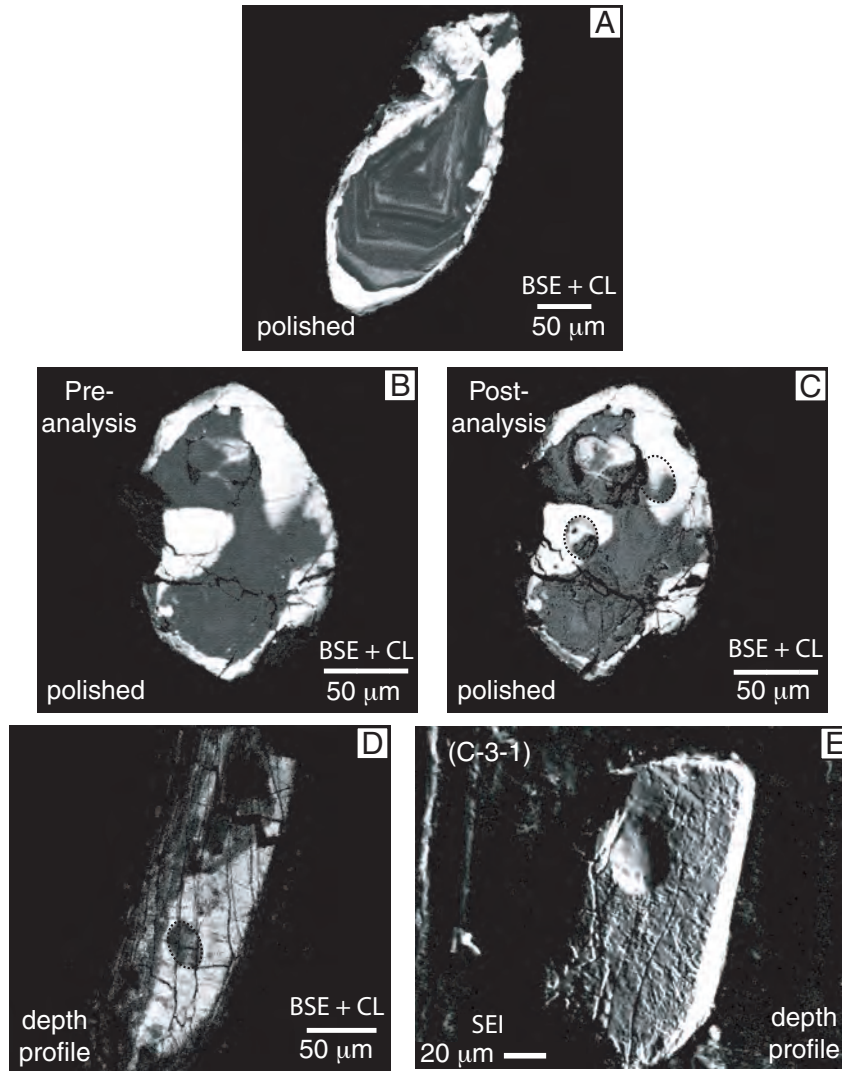

FIGURE 8. Cathodoluminescence (CL), Backscattered Electron (BSE), and Secondary Electron (SE) images of polished-grain and depth-profiled zircon crystals. **(A-B)**. Pre-analysis, overlain CL and BSE images of polished-grain zircon crystals from vein selvage. In A, oscillatory zoned igneous zircon core truncated by highly luminescent, irregular rim. In B, dark unzoned core surrounded by bright, irregular rim. C-D. Post-analysis, overlain CL and BSE images: **(C)** Same polished-grain selvage zircon as shown in B; **(D)** Depth-profiled zircon from little-altered schist. In both **C** and **D** ion microprobe pits marked by dotted ellipses. Note thin nature of brightly luminescent surfaces as seen from analysis pits drilled through thin bright surface into dark zircon below. **(E)**. SE grain surface image of selvage zircon C-3-1. Elliptical feature at upper left part of zircon is ion microprobe pit. Note irregular, etched, and cracked appearance of zircon crystal surface.

and garnet growth in Barrow's garnet zone in northeast Scotland. Sub-micrometer-scale depth-profiling of altered zircon thus provides a unique opportunity to determine precisely the timing of metamorphic fluid infiltration and metasomatism.

Uniform, highly discordant zircon subsurface regions

In zircon crystals from both the selvage and little-altered schist, only grains with Archean cores and uniform, highly discordant subsurface domains underwent significant isotopic alteration during Paleozoic fluid infiltration and metamorphism (Figs. 5A, 5B, and 5C; Figs. 6A, 6B, 6C, and 6D). The ~1000 Ma zircon crystals show little or no indication of alteration. Polished-grain zircon analyses indicate that oscillatory zonation and concordant U-Pb ages are common in the older grain cores (Figs. 4A and Fig. 8A). However, the deepest penetration of depth-profile analysis into an Archean zircon (~4.3 μm) records an unzoned grain subsurface with a uniform, yet highly discordant cluster of isotopic ages (Fig. 4C). This discrepancy indicates that subsurface regions within the zircon crystals must have undergone pervasive Pb-loss at some time between igneous crystallization and metamorphic fluid-induced alteration. Discordant results that plot entirely between the upper and lower concordia intercepts most likely reflect recrystallization of radiation-damaged regions and incomplete re-incorporation

of radiogenic Pb into the new, unzoned, homogenous zircon crystals (Mezger and Krogstad 1997). Subsurface discordance is common in grains with Archean-aged cores (Figs. 6A, 6B, 6C, and 6D; Figs. 8B and 8C), but absent in ~1000 Ma grains (Figs. 5A and 5B), strongly supporting the hypothesis of Mezger and Krogstad (1997), mentioned above.

Fluid-induced isotopic alteration and zircon growth/recrystallization

We have interpreted isotopic alteration of zircon crystals from Barrow's garnet zone to be the result of interaction with infiltrating metamorphic fluids. The presence and flow of fluids through Dalradian rocks during Barrovian metamorphism in northeast Scotland has been established previously by Ague (1997) and Dempster et al. (2000). The alteration that we observe is limited to fluid-accessible grain surfaces and through-going fractures within zircon crystals. Natural crystal surfaces of altered grains have distinct, pitted appearances that resemble hydrothermal etching textures (Fig 8E). Relatively non-fractured, subsurface regions of the grains would have been impermeable to infiltrating fluids and likewise show no evidence for Paleozoic alteration. Furthermore, isotopic alteration in zircon grains collected adjacent to the cross-cutting metamorphic quartz vein is significantly more intense and penetrates deeper into the grains than in zircon crystals collected distal to the vein. This increase in alteration intensity with proximity to the vein strongly suggests that metamorphic fluids moving through the vein (Ague 1997) were responsible for the U-Pb shifts observed along surfaces and fractures in the zircon crystals.

Isotopic alteration can result in apparent Pb-loss and discordant U-Pb data in zircon through three main mechanisms: diffusion, leaching, and growth/recrystallization of zircon (Mezger and Krogstad 1997). Volume diffusion and leaching are not considered to be primary mechanisms for isotopic alteration in the zircon crystals studied. Altered, depth-profiled zircon crystals show U-Pb discordance, apparent radiogenic Pb loss, and sharp increases in U, Th, and ^{204}Pb near mineral surfaces and fractures as a result of Paleozoic fluid infiltration. Although diffusion and/or leaching can cause Pb loss and U-Pb discordance, both mechanisms fail to explain the associated enrichment in U, Th, and common Pb along grain boundaries and fractures (Figs. 7A, 7B, and 7C). Volume diffusion of U, Th, and common Pb into the grains seems particularly unlikely, as U and Th diffusion are orders of magnitude slower than Pb diffusion (Lee et al. 1997; Cherniak and Watson 2000).

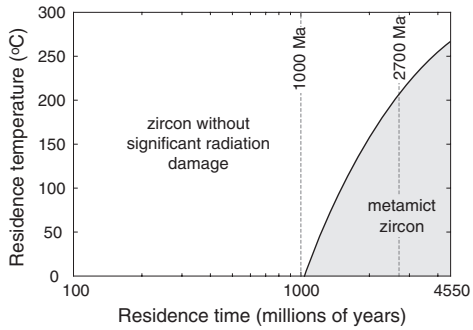

FIGURE 9. Residence temperature vs. time plot for metamictization of zircon with 100 ppm U calculated from expressions of Meldrum et al. (1998). Dashed lines at 1000 Ma and 2700 Ma indicate dominant subsurface and core age populations of zircon crystals from study sample. Zircon crystals with 100 ppm U must reside at ≤ 25 °C for > 1000 Ma to reach metamict state (gray region) (Cherniak and Watson 2000), indicating that 1000 Ma grains were most likely not highly radiation damaged at the time of metamorphic fluid infiltration (~462 Ma), but the Archean grains could have been. Note, however, that at temperatures of 500–550 °C, excessive radiation damage (denoted by gray area) is unlikely to accumulate in zircon crystals (Tagami et al. 1990; Weber et al. 1994).

Sub-micrometer-scale growth/recrystallization of zircon along crystal surfaces and fractures in preexisting zircon grains is the most likely cause of the observed isotopic alteration. CL, SE, and BSE imaging of zircon textures indicate that isotopic alteration was restricted to a thin, sharply defined zone of uniformly high luminescence along the outermost surface of the crystals (Figs. 8C and 8D). Well-defined alteration boundaries are consistent with the growth/recrystallization of zircon (Figs. 8A and 8B).

Zircon growth/recrystallization appears to have been limited to Archean grains. Unlike the ~1000 Ma zircon crystals that likely avoided significant radiation damage, the Archean grains could have undergone some degree of metamictization (Fig. 9; Meldrum et al. 1998; Cherniak and Watson 2000). However, at temperatures higher than ~500 °C, experiments suggest that most zircon crystals do not retain significant radiation damage (Fig. 9; Tagami et al. 1990; Weber et al. 1994) Thus, the correlation between fluid alteration and radiation damage is uncertain. The fractured and pitted surfaces of the Archean zircon crystals, however, represent a significant amount of reactive surface area that likely would have enhanced the growth/recrystallization process. Although the source of Zr incorporated into the new zircon is unknown, it could have originated easily from fluid-mediated local redistribution along zircon grain surfaces. A less likely but possible source of Zr may have been local breakdown of silicate phases that contained trace Zr (muscovite and chloritoid). Long-scale transport of Zr seems unlikely to us in light of experimental evidence (Ayers and Watson 1991) that indicates that Zr solubility in typical metamorphic fluids is very limited.

It is generally thought that zircon should largely exclude radiogenic Pb at the locus of new growth/recrystallization. C-3-1 and other depth-profile analyses in zircon crystals adjacent to the quartz vein that show concordant Paleozoic ages for the outer 0.1 μm of the grains (Figs. 6B and 6D) are consistent with this notion. However, in spite of the apparent incompatibility of Pb in zircon, common Pb (represented by ^{204}Pb) has been postulated to represent an indicator of "wet metamorphic" zircon growth conditions (Watson et al. 1997). For zircon crystals from the selvage, concentrations of common Pb along grain surfaces and are as much as an order of magnitude larger than concentrations in zircon subsurface regions (Fig. 7C). The fact that ^{197}Au intensity (a proxy for surface contamination) decreases sharply at the onset of the depth profile experiments indicates that the elevated ^{204}Pb levels we observe in the depth profiles (e.g., along internal fractures; Fig. 7C) are not the result of surface contamination. Considerable increases in ^{204}Pb without the incorporation of radiogenic Pb at crystal surfaces and in fractures could indicate

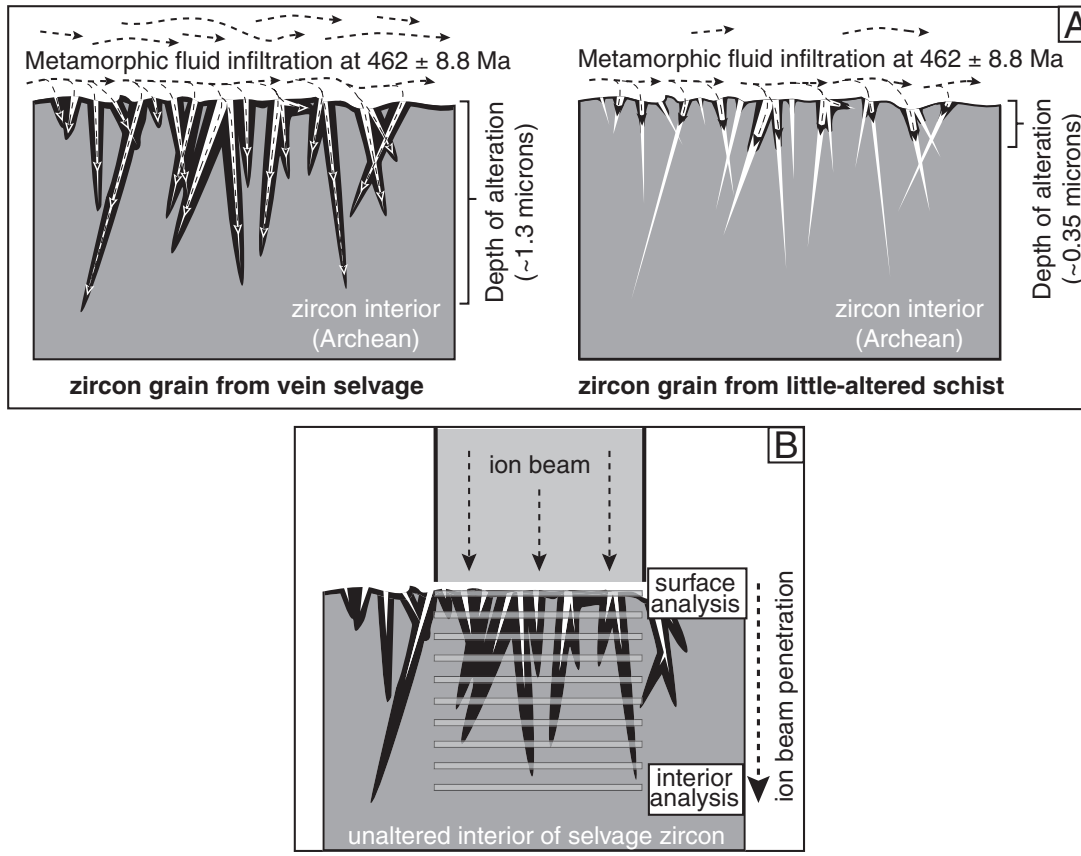

FIGURE 10. Schematic diagrams of fluid-zircon interactions and ion microprobe analysis. **(A)**. Pitted and fractured crystal surfaces of zircon crystals from the vein selvage and little-altered schist would have undergone different degrees of isotopic alteration due to variations in fluid infiltration (dashed lines). Larger fluxes adjacent to veins likely caused growth/recrystallization of new zircon (black areas) to deeper levels (~1.3 μm) in fractured grain surfaces of zircon crystals from the selvage relative to zircon crystals distal to veins (~0.35 μm) where fluxes would have been more limited. **(B)**. Vertically incident, depth-profiling ion beam averages isotopic composition of grain surface across beam diameter. At grain surface, beam only encounters altered zircon (black), thus reporting concordant Paleozoic alteration age. As analysis and ion beam penetration continues down into grain interior, measured isotopic compositions consist of mixture of newly grown/recrystallized Paleozoic zircon in pits and fractures (black) and host Archean zircon (gray) in variable proportions. As fractures and pits narrow within grain, isotopic composition approaches that of "unaltered" subsurface zircon. At deepest subsurface analysis, measured composition is that of host zircon. Resultant isotopic and geochemical data indicate smooth discordant arrays from crystal surface inward to grain subsurface (Figs. 4C and 4D; Figs. 6A, 6B, 6C, and 6D; Figs. 7A, 7B, and 7C).

that Pb did not diffuse into and out of the crystal, but was instead incorporated into the neoformed zircon. Lead would have been available for incorporation into the newly grown/recrystallized zircon because it was actively transported by the infiltrating fluids and significantly enriched in the metasediments adjacent to the quartz vein in our study sample (Fig. 3). We believe that this study could represent the first field-based example of common Pb in zircon as an indicator of metamorphic fluid infiltration and volatile-rich metamorphic conditions.

The depth-profile analysis indicate smooth, continuous variations in isotopic and chemical compositions inward from the zircon grain surfaces (Figs. 6A, 6B, 6C, and 6D; 7A, 7B and 7C). For zircon growth/recrystallization, it might be expected that the profiles should be more step-like with distinct domains of new zircon sharply separated from older zircon subsurface regions. Although the lack of such abrupt transitions could reflect inadequate depth resolution in our analysis, it could also indicate important multidimensional variation in the form of irregular interfaces produced by local fluid-zircon reactions at grain boundaries and in fractures.

Fluid-altered zircon crystals collected from our sample show very irregular, pitted surfaces with abundant fractures and microcracks that penetrate the grains to various depths (Fig. 8E; Fig. 10A). Isotopic alteration was concentrated along these pitted surfaces and within the fractures, producing a similarly irregular distribution of newly grown/recrystallized zircon. During depth-profile analysis, the ion microprobe beam was incident vertically upon the zircon surface and sputtered material across an elliptically shaped spot 30–40 µm in diameter (Fig. 10B), resulting in mechanical mixing of all zircon heterogeneities within that spot volume (note that a field aperture smaller than the diameter of the primary beam was employed to exclude secondary ions derived from the periphery of the ion pits). The time- and depth-integrated analysis continued into the zircon in the same manner. We envi-

sion that as the analysis moved deeper into the grains, newer Paleozoic zircon occurring in gradually narrowing fractures was mixed analytically in various proportions with unaltered zircon to produce a discordant array of isotopic data from the surface to the deepest analysis. Likewise, smooth, continuous changes in U, Th, and ^{204}Pb concentrations with depth are almost certainly the result of analytical mixing of Paleozoic zircon in fractures and pits with older, unaltered subsurface zircon. Larger fluid fluxes likely interacted with zircon crystals in the selvage adjacent to the fluid conduit (quartz vein) resulting in fluid infiltration and zircon growth/recrystallization to deeper levels within the fractured grain surface, whereas more-limited fluid fluxes distal to the vein resulted in significantly shallower grain penetration by metamorphic fluids (Fig. 10A). Variations in the depths at which peak U and Th concentrations are observed suggest continuously evolving elemental fluid compositions and varying fluid concentrations of U and Th available at each increment of zircon growth/recrystallization (Figs. 7A and 7B).

Comments on metamorphic fluid infiltration and regional tectonics

Recent age estimates for peak Barrovian metamorphism in northeast Scotland have converged to ~467–464 Ma. Our age estimate of 462 ± 8.8 Ma for fluid infiltration and isotopic alteration of zircon is consistent with the assertion that fluid metasomatism and metamorphism were contemporaneous in Barrow's garnet zone. The source of the fluids is uncertain, but some evidence suggests that dehydration of a subducting slab beneath the Dalradian metasediments may be a viable source. Remnants of sea floor-altered basalt are found within a dismembered ophiolite in the Highland Boundary Fault sequence, suggesting that an oceanic slab may have been subducted beneath the Dalradian (Bluck et al. 1980; Oliver et al. 2000). An age estimate for the Ballantrae Ophiolite Complex of 478 ± 8.0 Ma (Armstrong et al. 1999; Oliver et al. 2000) is consistent with the presence of a slab beneath northeast Scotland at or near the time of Barrovian metamorphism. Fluid-induced chemical changes in K, Na, and Ca described by Ague (1997) for Barrow's garnet zone are nearly identical to recent findings for accretionary metasediments in New Zealand, where Breeding and Ague (2002) documented dehydration of a downgoing slab as the fluid source for quartz-vein-forming metamorphic fluids that infiltrated overlying metasediments. Baxter et al. (2002) found that advective heat transport by magmas drove peak metamorphism in Barrow's garnet, kyanite, and sillimanite zones. Consequently, infiltration of fluids derived from, or equilibrated with, these magmas may have also caused the alteration of zircon described herein.

Concluding remarks

A growing body of work on volatile-rock interactions during metamorphism has indicated that fluid flow and elemental mass transport play critical roles in the chemical, isotopic, and deformational development of most crustal metamorphic terranes. Despite this intense focus on metamorphic fluids, precise ages for the timing of fluid infiltration remain difficult to obtain. Using depth-profile zircon SIMS analyses, we presented a precise metamorphic fluid infiltration age of 462 ± 8.8 Ma for Barrow's classic garnet zone in the Dalradian metasediments of northeast Scotland. The fluid infiltration age is identical (within error) to recent peak metamorphic garnet growth ages for the region, indicating that fluid infiltration accompanied Barrovian metamorphism. SIMS analyses of conventionally sectioned and polished zircon crystals affirm the timing of fluid influx and document Archean zircon ages for the Dalradian, perhaps indicating contributions from a Lewisian/Scourian source terrane. Metamorphic fluid infiltration resulted in the submicrometer- to micrometer-scale growth/recrystallization of high-U, high-Th zircon along crystal surfaces and fractures in preexisting Archean zircon grains. The fluid-induced zircon growth/recrystallization occurred at relatively low temperatures of 500–550 °C and incorporated significant concentrations of common Pb, thus providing the first field-based evidence for common Pb as an indicator of volatile-rich metamorphic conditions.

Acknowledgments

We thank J. Eckert for assistance with electron microprobe analysis, J. Greenwood for assistance with sample preparation and interferometry pit imaging, K. McKeegan for assistance during ion microprobe sessions, C.J. Carson and D.E. Wilbur for helpful discussions, and J.C. Ayers, C.P. Chamberlain, and G. Gehrels for thoughtful, constructive reviews. Support from National Science Foundation grants EAR-9405889, EAR-9810089, EAR-0001084, and EAR-0105927 (Ague) and EAR-0113563 (Grove) is gratefully acknowledged.

References cited

Ague, J.J. (1994) Mass transfer during Barrovian metamorphism of pelites, south-central Connecticut. II: Channelized fluid flow and the growth of staurolite and kyanite. American Journal of Science, 294, 1061–1134.

———(1997) Crustal mass transfer and index mineral growth in Barrow's garnet zone, northeast Scotland. Geology, 25, 73–76.

Ague, J.J., Baxter, E.F., and Eckert, J.O. (2001) High f_{O_2} during sillimanite zone metamorphism of part of the Barrovian type locality, Glen Clova. Scotland. Journal of Petrology, 42, 1301–1320.

Armstrong, H.A., Owen, A.W., and Floyd, J.D. (1999) Rare earth geochemistry of Arenig cherts from the Ballantrae Ophiolite and Leadhills imbricate zone, southern Scotland; implications for origin and significance to the Caledonian Orogeny. Journal of the Geological Society of London, 156, 549–560.

Atherton, M.P. (1977) The metamorphism of the Dalradian rocks of Scotland. Scottish Journal of Geology, 13, 331–370.

Ayers, J.C. and Watson, E.B. (1991) Solubility of apatite, monazite, zircon, and rutile in supercritical aqueous fluids with implications for subduction zone geochemistry. Philosophical Transactions of the Royal Society of London, A, 335, 365–375.

Barrow, G. (1893) On an intrusion of muscovite-biotite gneiss in the south-east highlands of Scotland and its accompanying metamorphism. Geological Society of London Quarterly Journal, 49, 330–358.

———(1898) On the occurrence of chloritoid in Kincardineshire. Geological Society of London Quarterly Journal, 54, 149–156.

——— (1912) On the geology of the lower Dee-side and the southern Highland border. Proceedings of the Geologist's Association, 23, 268–284.

Baumgartner, L.P. and Ferry, J.M. (1991) A model for coupled fluid-flow and mixed-volatile mineral reactions with applications to regional metamorphism. Contributions to Mineralogy and Petrology, 106, 273–285.

Baxter, E.F., Ague, J.J., and DePaolo, D.J. (2002) Prograde temperature-time evolution in the Barrovian type-locality constrained by Sm/Nd garnet ages from Glen Clova, Scotland. Journal of the Geological Society, London, 159, 71–82.

Bickle, M.J. (1992) Transport mechanisms by fluid-flow in metamorphic rocks: Oxygen and strontium decoupling in the Trois Seigneurs massif-A consequence of kinetic dispersion? American Journal of Science, 292, p. 289–316.

Bluck, B.J., Halliday, A.N., Aftalion, M., and Macintyre, R.M. (1980) Age and origin of the Ballantrae ophiolite and its significance to the Caledonian orogeny and the Ordovician time scale. Geology, 8, 492–495.

Breeding, C.M. and Ague, J.J. (2002) Slab-derived fluids and quartz vein formation in an accretionary prism, Otago Schist, New Zealand. Geology, 30, 499–502.

Breeding, C.M., Ague, J.J., Bröcker, M., and Bolton, E. (2003) Blueschist preservation in a retrograded, high-pressure, low-temperature metamorphic terrane, Tinos, Greece: Implications for fluid flow paths in subduction zones. Geochemistry, Geophysics, Geosystems, 4 (1), 9002, doi: 10.1029/2002GC000380.

Carson, C.J., Ague, J.J., Grove, M., Coath, C.D., and Harrison, T.M. (2002) U-Pb isotopic behaviour of zircon during upper-amphibolite facies fluid infiltration in the Napier Complex, east Antarctica. Earth and Planetary Science Letters, 199, 287–310.

Cawood, P.A., Nemchin, A.A., Smith, M., and Loewy, S. (2003) Source of Dalradian

Supergroup constrained by U-Pb dating of detrital zircon and implications for the East Laurentian margin. Journal of the Geological Society, London, 160, 231–246.
Chamberlain, C.P. and Rumble, D. III (1988) Thermal anomalies in a regional metamorphic terrane; an isotopic study of the role of fluids. Journal of Petrology, 29, 1215–1232.
Chamberlain, C.P., Zeitler, P.K., Barnett, D.E., Winslow, D., Poulson, S.R., Leahy, T., and Hammer, J.E. (1995) Active hydrothermal systems during the recent uplift of Nanga Parbat, Pakistan Himalaya. Journal of Geophysical Research, 100, 439–453.
Cherniak, D.J. and Watson, E.B. (2000) Pb diffusion in zircon. Chemical Geology, 172, 5–24.
Chinner, C.A. (1967) Chloritoid, and the isochemical character of Barrow's zones. Journal of Petrology, 8, 268–1282.
Compston, W., Williams, I.S., and Meyer, C.E. (1984) U-Pb geochronology of zircon crystals from lunar breccia 73217 using a sensitive high mass-resolution ion microprobe. Journal of Geophysical Research, 89, 525–534.
Connelly, J.N. (2000) Degree of preservation of igneous zonation in zircon as a signpost for concordancy in U/Pb geochronology. Chemical Geology, 172, 25–39.
Dempster, T.J., Fallick, A.E., and Whittemore, C.J. (2000) Metamorphic reactions in the biotite zone, eastern Scotland: high thermal gradients, metasomatism and cleavage formation. Contributions to Mineralogy and Petrology, 138, 348–363.
Dipple, G.M. and Ferry, J.M. (1992) Metasomatism and fluid flow in ductile fault zones. Contributions to Mineralogy and Petrology, 112, 149–164.
Droop, G.T.R. and Harte, B. (1995) The effect of Mn on the phase relations of medium-grade pelites: Constraints from natural assemblages on petrogenetic grid topology. Journal of Petrology, 36, 1549–1578.
Grove, M. and Harrison, T.M. (1999) Monazite Th-Pb age depth profiling. Geology, 27, 487–490.
Hanchar, J.M. and Rudnick, R.L. (1995) Revealing hidden structures: The application of cathodoluminescence and back-scattered electron imaging to dating zircons from lower crust xenoliths. Lithos, 36, 289–303.
Harte, B., Booth, J.E., Dempster, T.J., Fettes, D.J., Mendum, J.R., and Watts, D. (1984) Aspects of the post-depositional evolution of Dalradian and Highland Border Complex rocks in the Southern Highlands of Scotland. Transactions of the Royal Society of Edinburgh: Earth Sciences, 75, 151–163.
Högdahl, K., Gromet, L.P., and Broman, C. (2001) Low *P-T* Caledonian resetting of U-rich Paleoproterozoic zircons, central Sweden. American Mineralogist, 86, 534–546.
Ingebritsen, S.E. and Manning, C.E. (1999) Geological implications of a permeability-depth curve for the continental crust. Geology, 27, 1107–1110.
Konzett, J., Armstrong, R.A., Sweeney, R., and Compston, W. (1998) The timing of MARID metasomatism in the Kaapvaal mantle: An ion probe study of zircons from MARID xenoliths. Earth and Planetary Science Letters, 160, 133–145.
Lee, J.K.W., Williams, I.S., and Ellis D.J. (1997) Pb, U and Th diffusion in natural zircon. Nature, 390, 159–162.
Ludwig, K.R. (2001) User's Manual for Isoplot/Ex, v2.49, A Geochronological Toolkit for Microsoft Excel. Geochronological Centre Special Publication, 1a, 58 p. Berkeley, CA.
Luttge, A., Bolton, E.W., and Lasaga, A.C. (1999) An interferometric study of the dissolution kinetics of anorthite: The role of reactive surface area. American Journal of Science, 299, 652–678.
Meldrum, A., Boatner, L.A., Weber, W.J., and Ewing, R.C. (1998) Radiation damage in zircon and monazite. Geochimica et Cosmochimica Acta, 62, 2509–2520.
Mezger, K. and Krogstad, E.J. (1997) Interpretation of discordant U-Pb zircon ages: An evaluation. Journal of Metamorphic Geology, 15, 127–140.
Mojzsis, S.J. and Harrison, T.M. (2002) Establishment of a 3.83-Ga magmatic age for the Akilia tonalite (southern West Greenland). Earth and Planetary Science Letters, 202, 563–576.
Oliver, G.J.H. (2001) Reconstruction of the Grampian episode in Scotland: its place in the Caledonian Orogeny. Tectonophysics, 332, 23–49.
Oliver, G.J.H., Chen, F., Buchwaldt, R., and Hegner, E. (2000) Fast tectonometamorphism and exhumation in the type area of the Barrovian and Buchan zones. Geology, 28, 459–462.
Paces, J.B. and Miller, J.D. (1993) Precise U-Pb ages of Duluth Complex and related mafic intrusions, northeastern Minnesota: Geochronological insights to physical, petrogenetic, paleomagnetic, and tectonomagmatic processes associated with the 1.1 Ga Midcontinent Rift System. Journal of Geophysical Research, 98, 13997–14013.
Rumble, D., Ferry, J.M., Hoering, T.C., and Boucot, A.J. (1982) Fluid flow during metamorphism at the Beaver Brook fossil locality. American Journal of Science, 282, 886–919.
Rye, D.M. and Rye, R.O. (1974) Homestake Gold Mine, South Dakota; I, Stable Isotope Studies. Economic Geology, 69, 293–317.
Rye, R.O., Schuiling, R.D., Rye, D.M., and Jansen, J.B.H. (1976) Carbon, hydrogen, and oxygen isotope studies of the regional metamorphic complex at Naxos, Greece. Geochimica et Cosmochimica Acta, 40, 1031–1049.
Sinha, A.K., Wayne, D.M., and Hewitt, D.A. (1992) The hydrothermal stability of zircon: Preliminary experimental and isotopic studies. Geochimica et Cosmochimica Acta, 56, 3551–3560.
Stacey, J.S. and Kramers, J.D. (1975) Approximation of terrestrial lead isotope evolution by a two-stage model. Earth and Planetary Science Letters, 26, 207–221.
Tagami, T., Ito, H., and Nishimura, S. (1990) Thermal annealing characteristics of spontaneous fission tracks in zircon. Chemical Geology, 80, 159–169.
Watson, E.B., Cherniak, D.J., Hanchar, J.M., Harrison, T.M., and Wark, D.A. (1997) The incorporation of Pb into zircon. Chemical Geology, 141, 19–31.
Weber, W.J., Ewing, R.C., and Wang, L-M. (1994) The radiation-induced crystalline-to-amorphous transition in zircon. Journal of Materials Research, 9, 688–698.
Wing, B.A. and Ferry, J.M. (2003) Three-dimensional geometry of metamorphic fluid flow during Barrovian regional metamorphism from an inversion of combined petrologic and stable isotopic data. Geology, 30, 639–642.
Yardley, B.W.D. and Bottrell, S.H. (1992) Silica mobility and fluid movement during metamorphism of the Connemara schists, Ireland. Journal of Metamorphic Geology, 10, 453–464.
Zeitler, P.K., Sutter, J.F., Williams, I.S., Zartman, R.E., and Tahirkheli, R.A.K. (1989) Geochronology and temperature history of the Nanga Parbat-Haramosh Massif, Pakistan. Geological Society of America Special Paper, 232, 1–22.

MANUSCRIPT RECEIVED SEPTEMBER 17, 2003
MANUSCRIPT ACCEPTED MARCH 8, 2004
MANUSCRIPT HANDLED BY GRAY BEBOUT